Magnetization properties of some quantum spin ladders

Kunj Tandon
Solid State and Structural Chemistry Unit, Indian Institute of Science, Bangalore 560012, India

Siddhartha Lal
Department of Physics, Indian Institute of Science, Bangalore 560012, India

Swapan K. Pati and S. Ramasesha
Solid State and Structural Chemistry Unit, Indian Institute of Science, Bangalore 560012, India

Diptiman Sen
Centre for Theoretical Studies, Indian Institute of Science, Bangalore 560012, India

(Received 19 June 1998)

The experimental realization of various spin ladder systems has prompted their detailed theoretical investigations. Here we study the evolution of ground-state magnetization with an external magnetic field for two different antiferromagnetic systems: a three-legged spin-1/2 ladder, and a two-legged spin-1/2 ladder with an additional diagonal interaction. The finite system density-matrix renormalization-group method is employed for numerical studies of the three-chain system, and an effective low-energy Hamiltonian is used in the limit of strong interchain coupling to study the two- and three-chain systems. The three-chain system has a magnetization plateau at one-third of the saturation magnetization. The two-chain system has a plateau at zero magnetization due to a gap above the singlet ground state. It also has a plateau at half of the saturation magnetization for a certain range of values of the couplings. We study the regions of transitions between plateaus numerically and analytically, and find that they are described, at first order in a strong-coupling expansion, by an XXZ spin-1/2 chain in a magnetic field; the second-order terms give corrections to the XXZ model. We also study numerically some low-temperature properties of the three-chain system, such as the magnetization, magnetic susceptibility and specific heat. [S0163-1829(99)03001-5]

I. INTRODUCTION

One-dimensional and quasi-one-dimensional quantum spin systems have been studied extensively in recent years for several reasons. Many such systems have been realized experimentally, and a variety of theoretical techniques, both analytical and numerical, are available to study the relevant models. Due to large quantum fluctuations in low dimensions, such systems often have unusual properties such as a gap between a singlet ground state and the excited nonsinglet states; this leads to a magnetic susceptibility which vanishes exponentially at low temperatures. Perhaps the most famous example of this is the Haldane gap which was predicted theoretically in integer spin Heisenberg antiferromagnetic chains,[1] and then observed experimentally in a spin-1 system $Ni(C_2H_8N_2)_2NO_2(ClO_4)$.[2] Other examples include the spin ladder systems in which a small number of one-dimensional spin-1/2 chains interact amongst each other.[3] It has been observed that if the number of chains is even, i.e., if each rung of the ladder (which is the unit cell for the system) contains an even number of spin-1/2 sites, then the system effectively behaves like an integer spin chain with a gap in the low-energy spectrum. Some two-chain ladders which show a gap are $(VO)_2P_2O_7$,[4] $SrCu_2O_3$ (Ref. 5) and $Cu_2(C_5H_{12}N_2)_2Cl_4$.[6] Conversely, a three-chain ladder which effectively behaves like a half-odd-integer spin chain and does *not* exhibit a gap is $Sr_2Cu_3O_5$.[5] A related observation is that the quasi-one-dimensional system $CuGeO_3$ spontaneously dimerizes below a spin-Peierls transition temperature;[7] then the unit cell contains two spin-1/2 sites and the system is gapped.

The results for gaps quoted above are all in the absence of an external magnetic field. The situation becomes more interesting in the presence of a magnetic field.[8] Then it is possible for an integer spin chain to be gapless and a half-odd-integer spin chain to show a gap above the ground state for appropriate values of the field.[9–19] This has been demonstrated in several models using a variety of methods such as exact diagonalization of small systems, bosonization and conformal field theory,[20,21] and perturbation theory.[22] In particular, it has been shown that the magnetization of the system can exhibit plateaus at certain nonzero values for some finite ranges of the magnetic field. Further, for a Hamiltonian which is invariant under translation by one unit cell, the value of the magnetization per unit cell is quantized to be a rational number at each plateau.

The necessary (but not sufficient) condition for the magnetization quantization is given as follows.[9] Let us assume that the magnetic field points along the $\hat{z}$ axis, the total Hamiltonian H is invariant under spin rotations about that axis, and the maximum possible spin in each unit cell of the Hamiltonian is given by S. Consider a state ψ such that the expectation value of S_z per unit cell is equal to m_s in that state, and ψ has a period n, i.e., it is invariant only under translation by a number of unit cells equal to n or a multiple of n. (It is clear that if $n \geqslant 2$, then there must be n such states with the same energy, since H is invariant under a translation

 ©1999 The American Physical Society

by one unit cell). Then the quantization condition says that a magnetic plateau is possible at the state ψ, i.e., there is a range of values of the external field for which ψ is the ground state and is separated by a finite gap from states with slightly higher or lower values of total S_z, only if

$$n(S-m_s)=\text{an integer}. \tag{1}$$

This condition is very useful because it enables us to restrict our attention to some particular values of m_s and n when searching for possible plateaus in a given model. Note that the saturated state in which all spins point along the magnetic field trivially satisfies Eq. (1) since it has $m_s=S$ (or $-S$) and $n=1$.

In this paper, we will study the magnetization as a function of the applied field for a two- and three-chain ladder. We will do so both numerically, using the density-matrix renormalization-group method (DMRG),[23,24] and perturbatively, using a low-energy effective Hamiltonian (LEH).[15,25] Our analysis will extend the currently known results in many ways. We have used DMRG to study two-spin correlation functions in the ground state, and some finite-temperature thermodynamic properties such as magnetic susceptibility and specific heat. Further, our LEH goes up to the second order in a strong-coupling expansion. Whenever possible, we will use the analytical results from the LEH to understand the numerical results. The first-order LEH will turn out to be the well-studied XXZ spin-1/2 chain in a longitudinal magnetic field,[11,26] and it will usually prove to be sufficient for a qualitative understanding of the results. However, we will find it necessary to invoke the second-order results (which give corrections to the XXZ model) for a more accurate comparison with the numerics.

The paper is organized as follows. In Sec. II, we will present all the numerical results we have obtained for the three-chain ladder using DMRG. We will see that there is a finite energy gap and exponentially decaying spin correlations at each plateau, while there is no gap and the two-spin correlations decay as powers in between two plateaus. We will also study how the plateaus gradually disappear and how the susceptibility and specific heat evolve as we increase the temperature. In Sec. III, we will derive the LEH for the same model and show how it can be used to understand some of the numerical results in Sec. II. We will also derive the LEH for a two-chain ladder which can be thought of as a dimerized and frustrated spin-1/2 chain,[27] and we will use it to understand magnetization plateaus in the ground state. We will see that for certain values of the dimerization and frustration, the ground state can spontaneously break translation invariance leading to an additional plateau at an intermediate value of the magnetization. In Sec. IV, we will summarize our results and point out some directions for future studies.

II. DENSITY-MATRIX RENORMALIZATION-GROUP STUDY OF THE THREE-CHAIN LADDER

We have numerically studied a three-chain spin-1/2 ladder governed by the Hamiltonian

$$H=J'\sum_a\sum_n \mathbf{S}_{a,n}\cdot\mathbf{S}_{a+1,n} + J\sum_{a=1}^{3}\sum_n \mathbf{S}_{a,n}\cdot\mathbf{S}_{a,n+1}-h\sum_{a=1}^{3}\sum_n S^z_{a,n}, \tag{2}$$

where a denotes the chain index, n denotes the rung index, h denotes the magnetic field (we have absorbed the gyromagnetic ratio g and the Bohr magneton μ_B in the definition of h), and $J,J'>0$. For convenience, we choose $h\geqslant 0$ since the region $h<0$ can be deduced from it by reflection about the zero field. It is convenient to scale out the parameter J, and quote all results in terms of the two dimensionless quantities J'/J and h/J. If the length of each chain is L, the total number of sites is $N=3L$. Since the total S^z is a good quantum number, it is more convenient to do the numerical computations *without* including the magnetic-field term in Eq. (2), and then to add the effect of the field at the end of the computation. The label $n+1$ (or $a+1$) is appropriately interpreted for periodic boundary conditions along the chain (or rung).

For the ground-state properties, we have only considered an open boundary condition (OBC) in the rung direction, namely, the summation over a in the first term of Eq. (2) runs over 1,2. However, for low-temperature properties, we have studied both OBC, as well as a periodic boundary condition (PBC) in the rung direction in which we sum over $a=1,2,3$ in the first term. (Only the OBC is realized along the rungs in the experimental systems studied so far. However, PBC along the rungs is interesting for theoretical reasons as we will see below).

For small systems, we have performed exact diagonalization with periodic boundary conditions in the chain direction. For larger systems, we have done DMRG calculations (using the finite system algorithm[23]) with open boundary conditions in the chain direction. For exact diagonalization, we have gone up to 24 sites, i.e., a chain length of 8. With DMRG, we have gone up to 120 sites (chain length of 40) after checking that the DMRG and exact results match for 24 sites. The number of dominant density matrix eigenstates,

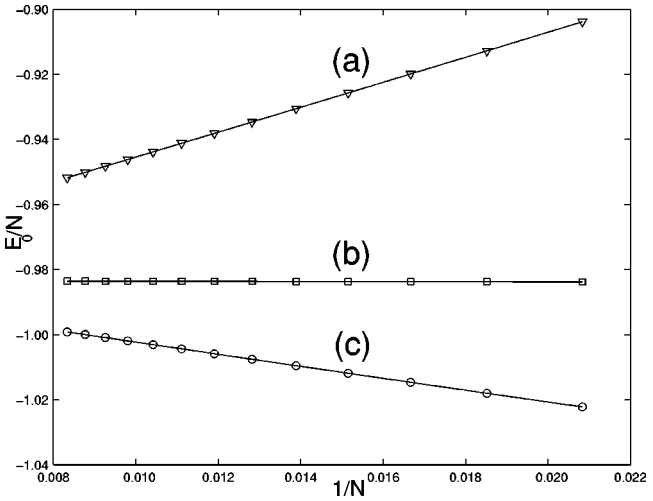

FIG. 1. The energy/site in units of J vs $1/N$ at the $m_s=1/2$ plateau, for $J/J'=1/3$. The curves indicate quadratic fits for (a) $E_0(M+1,N)$, (b) $E_0(M,N)$, and (c) $E_0(M-1,N)$.

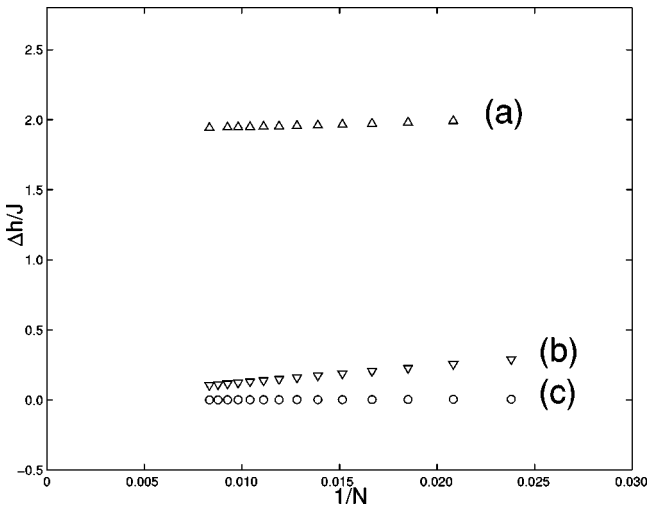

FIG. 2. Plateau widths vs $1/N$ for (a) $m_s=1/2$, (b) $m_s=0$, and (c) $m_s=1$.

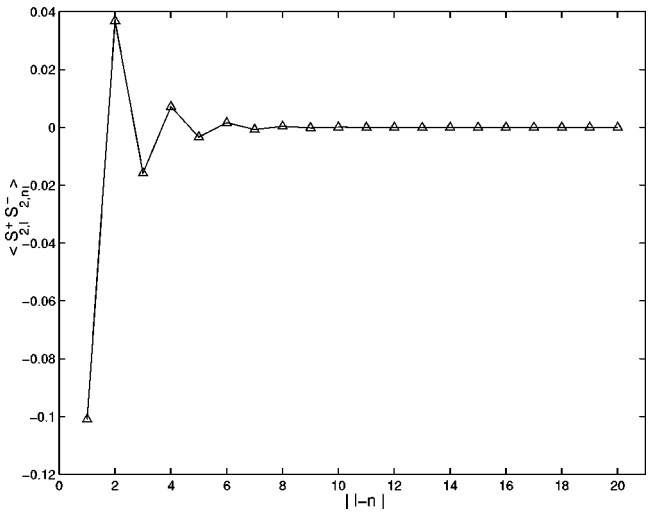

FIG. 4. Correlation function $\langle S^+_{2,l}S^-_{2,n}\rangle$ at the $m_s=1/2$ plateau for $J/J'=1/3$.

corresponding to the m largest eigenvalues of the density matrix, that we retained at each DMRG iteration was $m=80$. In fact, we varied the value of m from 60 to 100, and found that $m=80$ gives satisfactory results in terms of agreement with exact diagonalization for small systems and good numerical convergence for large systems. For inputting the values of the couplings into the numerical programs, it is more convenient to think of the system as a single chain (rather than as three chains) with the Hamiltonian

$$H=\frac{2}{3}J'\sum_i\left[1-\cos\left(\frac{2\pi i}{3}\right)\right]\mathbf{S}_i\cdot\mathbf{S}_{i+1}+J\sum_i\mathbf{S}_i\cdot\mathbf{S}_{i+3}. \tag{3}$$

The system is grown by adding two new sites at each iteration. Note that our method of construction ensures that we obtain the three-chain ladder structure after every third iteration when the total number of sites becomes a multiple of 6. At various system sizes, starting from 48 sites and going up to 120 sites in multiples of 6 sites, we computed the energies after doing three finite system iterations; we found that the energy converges very well after three iterations. The energy data is used in Figs. 1 and 2. After reaching 120 sites, we computed the spin densities and correlations after doing three finite system iterations. This data is used in Figs. 3–8.

All our numerical results quoted below are for $J/J'=1/3$. We chose this particular value of the ratio for two reasons; there is a particularly broad magnetization plateau at $m_s=1/2$ which can be easily found numerically, and that value of the ratio is sufficiently deep inside the strong-coupling regime that the second-order perturbation expansion of Sec. II gives results which compare very well with the numerics.

We now describe the various ground-state properties we have found with OBC along the rungs. We looked for a magnetization plateau as follows. Motivated by the conditions in Eq. (1), we looked for a plateau at $m_s=1/2$ which would correspond to $n=1$ in that equation, since $S=3/2$. We also looked for plateaus at $m_s=0$ and $m_s=1$, each of which would correspond to $n=2$, i.e., a doubly degenerate state which has a period of two rungs. For a system with N sites, a given value of magnetization per rung, m_s, corresponds to a sector with total S^z equal to $M=m_sN/3$. Using the infinite system algorithm, we found the lowest energies $E_0(S^z,N)$ in the three sectors $S^z=M+1$, M, and $M-1$. Then we examined the three plots of E_0/NJ versus $1/N$ and extrapolated the results up to the thermodynamic limit $N\to\infty$. We fitted these plots with the formula $E_0/NJ=e_i+a_i/N+b_i/N^2$, where the label $i=1,2,3$ denotes the S^z sectors $M+1$, M, and $M-1$. (We found that a quadratic fit in $1/N$ matches the data much better than just a linear fit). In the thermodynamic limit, the values of the three intercepts e_i should match since those are just the energy per site for the three states whose S_z's differ by only 1. However, the three slopes a_i are not equal in general. We now show that there is a magnetization plateau if $a_1+a_3-2a_2$ has a nonzero value. Since the three

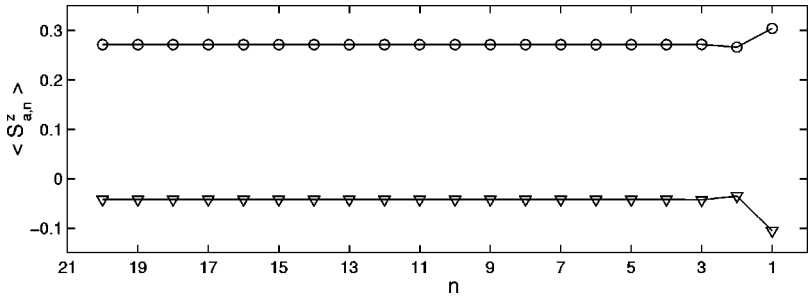

FIG. 3. Spin densities at the $m_s=1/2$ plateau for $J/J'=1/3$. The upper points (circles) denote the top chain $a=1$, while the lower points (triangles) denote the middle chain $a=2$. $n=1$ and 20 denote the end and middle rungs, respectively.

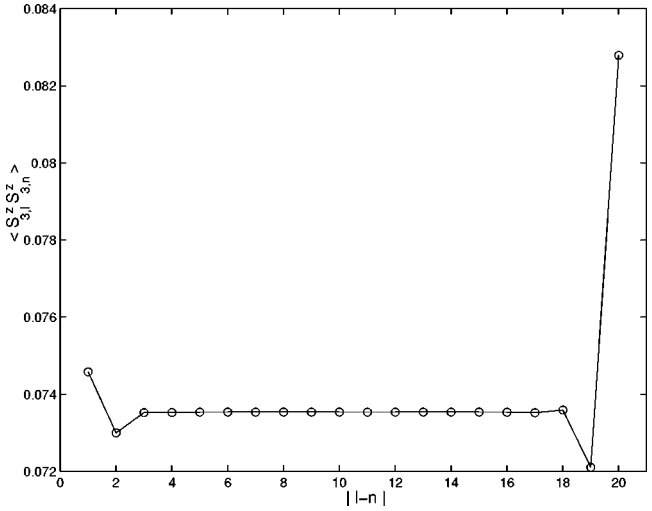

FIG. 5. Correlation function $\langle S^z_{1,l} S^z_{1,n} \rangle$ at the $m_s = 1/2$ plateau.

energies E_0 are computed without including the magnetic-field term, the upper critical field h_{c+} where the states with $S_z = M+1$ and M become degenerate is given by

$$h_{c+}(N) = E_0(M+1,N) - E_0(M,N). \tag{4}$$

Similarly, the lower critical field h_{c-} where the states with $S_z = M$ and $M-1$ become degenerate is given by

$$h_{c-}(N) = E_0(M,N) - E_0(M-1,N). \tag{5}$$

We therefore have a finite interval $\Delta h(N) = h_{c+}(N) - h_{c-}(N)$ in which the lowest energy state with $S^z = M$ is the ground state of the system with N sites in the presence of a field h. If this interval has a nonzero limit as $N \to \infty$, we have a magnetization plateau. Thus, in the thermodynamic limit, the plateau width $\Delta h/J$ is equal to $a_1 + a_3 - 2a_2$.

We will now quote our numerical results for $J/J' = 1/3$. For a rung magnetization of $m_s = 1/2$, i.e., $M = N/6$, we found the three slopes a_i to be equal to 3.77, -0.02, and -1.93; see Fig. 1. This gives the upper and lower critical fields to be

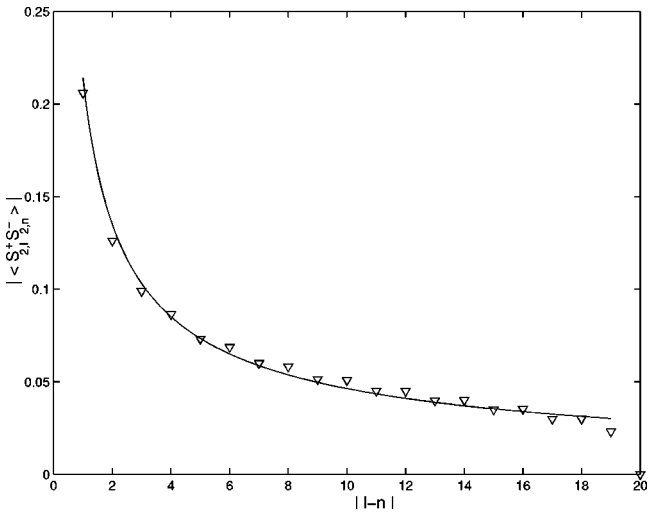

FIG. 6. Correlation functions $\langle S^+_{1,l} S^-_{2,n} \rangle$ in the $m_s = 1$ state for $J/J' = 1/3$.

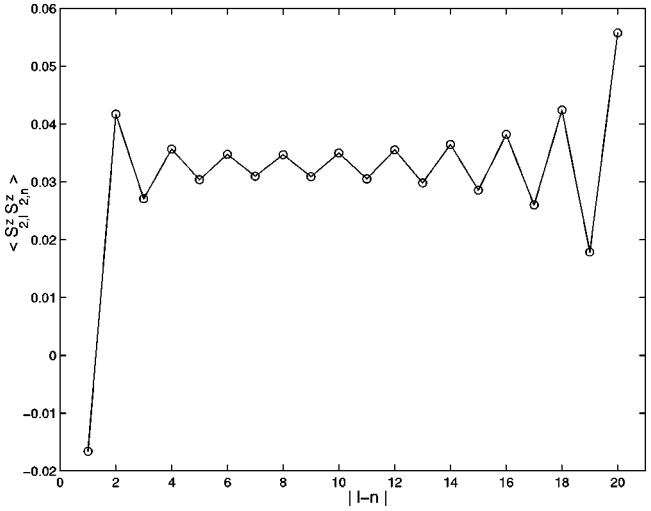

FIG. 7. Correlation function $\langle S^z_{2,l} S^z_{2,n} \rangle$ in the $m_s = 1$ state.

$$\frac{h_{c+}}{J} = a_1 - a_2 = 3.79, \quad \frac{h_{c-}}{J} = a_2 - a_3 = 1.91,$$

$$\frac{\Delta h}{J} = \frac{h_{c+} - h_{c-}}{J} = 1.88. \tag{6}$$

This is a sizable plateau width, and it agrees with the exact diagonalization results[10] and with the second-order perturbation expansion which will be discussed in the next section. For a rung magnetization of $m_s = 1$, we found the a_i to be equal to 4.97, -0.24, and -5.43. Thus the upper and lower critical fields are

$$\frac{h_{c+}}{J} = 5.21, \quad \frac{h_{c-}}{J} = 5.19, \quad \frac{\Delta h}{J} = 0.02. \tag{7}$$

Finally, for a rung magnetization of $m_s = 0$, we need the energies of states with $M = 0$ and $M = \pm 1$. Since the last two states must have the same energy, we have $a_1 = a_3$ and it is sufficient to plot only $E_0(0,N)$ and $E_0(1,N)$ versus $1/N$. We found a_1 and a_2 to be equal to 0.39 and 0.34. This gives the upper and lower fields to be

$$\frac{h_{c+}}{J} = 0.05, \quad \frac{h_{c-}}{J} = -0.05, \quad \frac{\Delta h}{J} = 0.10. \tag{8}$$

The plateau widths given in Eqs. (7) and (8) are rather small. In Fig. 2, we indicate the plateau widths $\Delta h(N)/J$ as a function of $1/N$ for $m_s = 1/2$, 0, and 1. We will see that the LEH in the next section actually predicts that there should be no plateaus at $m_s = 0$ and 1.

Next, we computed the various spin correlations for the 120-site system. We studied the spin densities $\langle S^z_{a,n} \rangle$ where the chain index $a = 1,2,3$ and n is the rung index. [Due to the rotation invariance about the $\hat{z}$ axis, the other two spin densities $\langle S^{\pm}_{a,n} \rangle$ must vanish.] For the plateau at $m_s = 1/2$, we found that

$$\langle S^z_{1,n} \rangle = \langle S^z_{3,n} \rangle = 0.27, \quad \langle S^z_{2,n} \rangle = -0.04, \tag{9}$$

for values of n in the middle of the system. The spin densities are shown in Fig. 3.

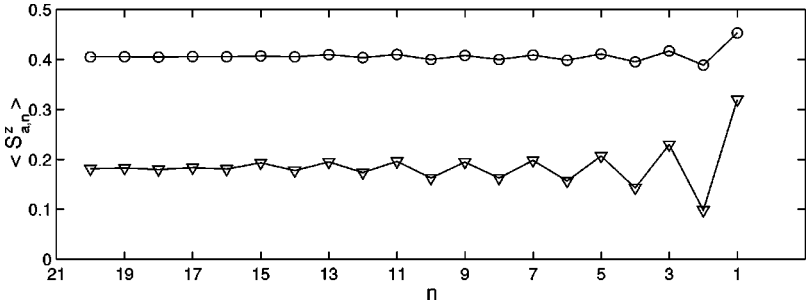

FIG. 8. Spin densities in the $m_s=1$ state for $J/J'=1/3$. The upper points (circles) denote the top chain $a=1$, while the lower points (triangles) denote the middle chain $a=2$. $n=1$ and 20 denote the end and middle rungs, respectively.

We also examined several two-spin correlations which can be denoted by $\langle S^z_{a,l}S^z_{b,n}\rangle$ and $\langle S^+_{a,l}S^-_{b,n}\rangle$. For the zz correlations, it is convenient to subtract the product of the two separate spin densities; the subtracted zz correlations then go to zero for large rung separations $|l-n|$, just like the $+-$ correlations. At $m_s=1/2$, we found that all these correlations decay very rapidly to zero as $|l-n|$ grows. In fact, the fall offs were so fast that we were unable to compute sensible correlation lengths. All the correlation lengths are of the order of one or two rungs as can be seen in Figs. 4 and 5.

On the other hand, for the state at $m_s=0$, we found that all the two-spin correlations decay quite slowly. The decays are consistent with power law fall offs of the form $A(-1)^{|l-n|}/|l-n|^{\eta}$. It is difficult to find η very accurately since the maximum value of $|l-n|$ is only 20; this is because we fixed one site to be in the middle of the chain (to minimize edge effects), and the maximum chain length is 40 for our DMRG calculations. For $m_s=0$, the exponent η for all the correlations was found to be around 1. There was no difference in the behaviors of the zz and $+-$ correlations since this was an isotropic system; $m_s=0$ is the ground state if the magnetic field is zero.

For the state at $m_s=1$ (which is the ground state only for a substantial value of the magnetic field), we found that the $+-$ correlations again decay quite slowly consistent with a power law. The exponents η for the different $+-$ correlations varied from 0.61 to 0.70 with an average value of 0.66; see Fig. 6 for an example. However, the zz correlations actually increased, rather than decreased, with increasing separation $|l-n|$; see Fig. 7. We found that this is because of large edge effects. Since the magnetic field is particularly strong for the state with $m_s=1$, and sites at the ends have fewer neighbors coupled antiferromagnetically to them, they respond more strongly to the magnetic field than sites near the center of the system. This can be seen from Fig. 8 where the spin density $S^z_{a,n}$ shows a sharp increase towards the end of the chain (the rung index n is equal to 1 at the end).

We now summarize the properties of the three states studied with OBC along the rungs. The state with $m_s=1/2$ is characterized by a large gap to excited states and extremely short correlation lengths for spin correlations. The states at $m_s=0$ and $m_s=1$ appear to have no gaps to excited states (within our numerical accuracy), and have slow fall offs of correlation functions consistent with power laws.

We now describe some low-temperature thermodynamic properties of the three-chain system obtained using DMRG. Although DMRG is normally expected to be most accurate for targeting the lowest states in different S^z sectors, earlier studies of mixed spin chains have shown that DMRG is quite reliable for computing low-temperature properties also.[28] There are two reasons for this; the low-lying excited states generally have a large projection onto the space of DMRG states which contains the ground state, and the low-lying excitations in one sector are usually the lowest states in nearby S^z sectors.

We first checked that for systems with 12 sites, the results obtained using DMRG agree well with those obtained by exact diagonalization. We then used DMRG to study the magnetization, susceptibility and specific heat of 36-site systems with both OBC and PBC along the rungs. We first compute the partition function $Z=\Sigma_i \exp[-\beta(E_i-h(S^z)_i)]$, where the sum is over all the states i in all the S^z sectors, and $\beta=1/k_BT$ where k_B is the Boltzmann constant. Then the magnetization is given by

$$\langle M\rangle=\frac{1}{Z}\sum_i (S^z)_i e^{-\beta[E_i-h(S^z)_i]}. \tag{10}$$

The magnetic susceptibility is related to the fluctuation in magnetization,

$$\chi=\beta[\langle M^2\rangle-\langle M\rangle^2], \tag{11}$$

and the specific heat is related to the fluctuation in energy,

$$\frac{C_V}{k_B}=\beta^2[\langle E^2\rangle-\langle E\rangle^2]. \tag{12}$$

The plots of magnetization versus magnetic field for various temperatures are shown in Figs. 9 and 10 for OBC and PBC, respectively, along the rungs. The temperature T is measured in units of J/k_B. We see that the plateau at $m_s=1/2$ disappears quite rapidly as we increase the temperature. With OBC along rungs, the plateau has almost disappeared at $T=0.4$ which is substantially lower than the width $\Delta h/J=1.88$. The plots of susceptibility in Fig. 11 for OBC also show no surprises. The susceptibility is (exponentially) small at low temperatures in the region of the plateau because the magnetic excitations there are separated from the ground state by a gap.

However, the specific heats shown in Figs. 12 and 13 demonstrate an interesting difference between OBC and PBC along the rungs. While it is very small at low temperatures for OBC, it is not small for PBC; further, it shows a plateau in the same range of magnetic fields as the magnetization

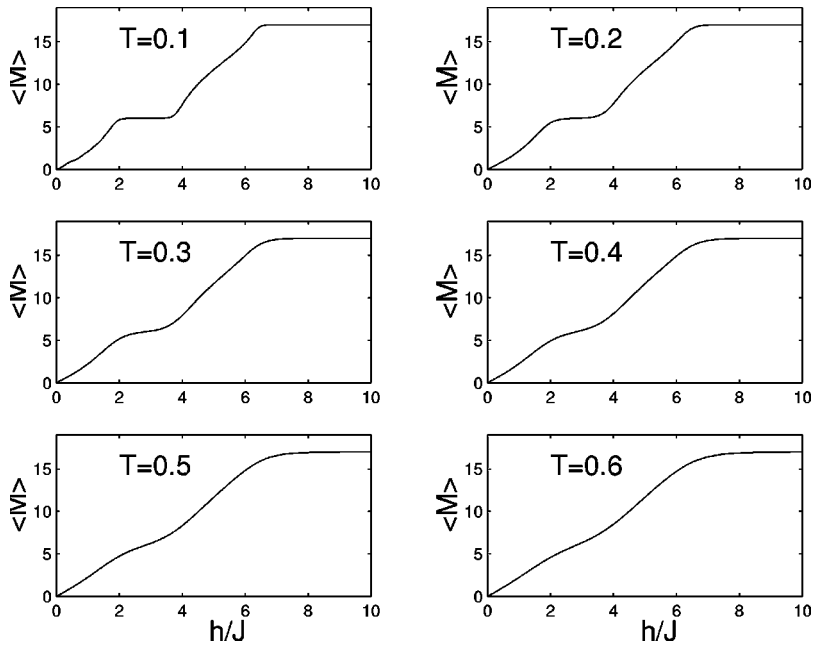

FIG. 9. Magnetization vs magnetic field for 36 sites, with OBC along rungs for $J/J'=1/3$.

itself. These two observations strongly suggest that the system with PBC along the rungs has *nonmagnetic* excitations which do not contribute to the magnetization or susceptibility, but do contribute to the specific heat. Figure 14 gives a more direct comparison between OBC and PBC along the rungs. The LEH of Sec. III will clearly show the origin of these excitations. Although these excitations were studied by previous authors,[10,11,24] we believe that our specific-heat plots prove their existence most physically. To show these excitations even more explicitly, we present in Fig. 15 all the energy levels for a 12-site chain in the sector $S^z=2$ (i.e., $m_s=1/2$) using exact diagonalization. It is clear that the ground state is well separated from the excited states for OBC, but it is at the bottom of a band of excitations for PBC; these excitations are nonmagnetic since they have the same value of S^z as the ground state.

We should point out that the rapid but small fluctuations seen in Figs. 11–14, in the susceptibility and specific heat at the lowest temperature of $T=0.1$, are due to finite-size effects. Apart from a large plateau at $m_s=1/2$, a system with only 36 sites also has small plateaus for several values of m at zero temperature. These lead to small wiggles in the magnetization $\langle M\rangle$ at very low temperature. The wiggles get amplified in the susceptibility since it is equal to the first derivative, i.e., $\chi=\partial\langle M\rangle/\partial h$. The specific heat shows low-temperature fluctuations for the same reason.

We should mention here that a small plateau has been found at $m_s=0$ for PBC along the rungs.[11,24] The half-width

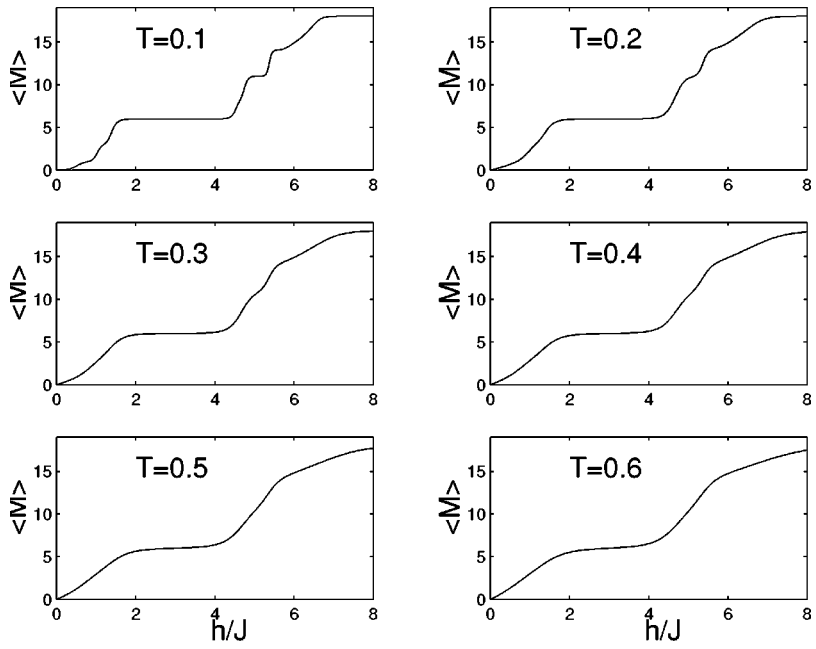

FIG. 10. Magnetization vs magnetic field for 36 sites, with PBC along rungs for $J/J'=1/3$.

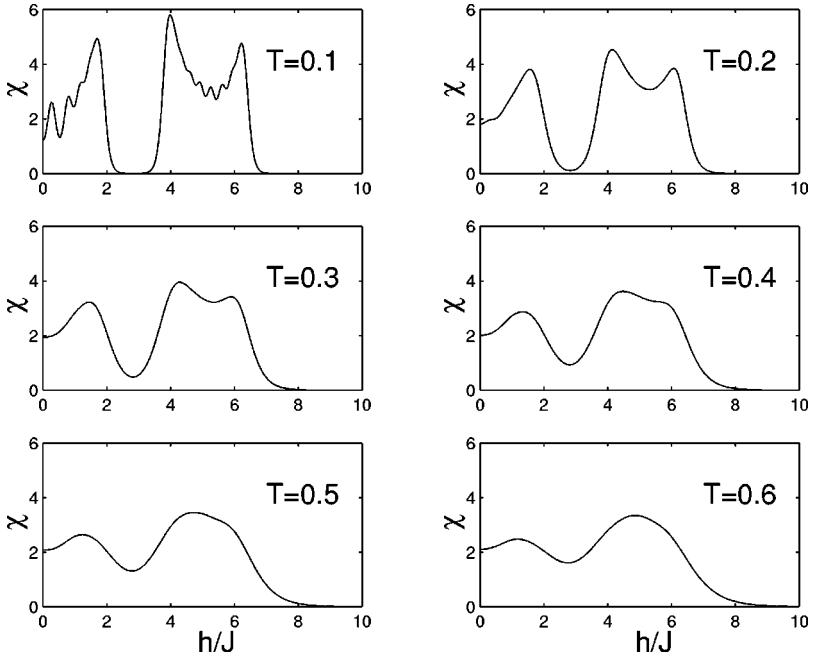

FIG. 11. Susceptibility vs magnetic field for 36 sites, with OBC along rungs.

is given by $h_{c+}/J=0.21$ in the limit $J'/J\to\infty$. However, this plateau is not clearly visible in our low-temperature plots of magnetization and susceptibility.

III. LOW-ENERGY EFFECTIVE HAMILTONIANS

A. General comments

We will now discuss the LEH approach for studying the properties of spin ladders. There are two possible limits which may be considered. One could examine $J'/J\to 0$ which corresponds to weakly interacting chains, and then directly use techniques from bosonization and conformal field theory; this has been done in detail by others.[10,11,14,15] We will therefore consider the strong-coupling limit $J/J'\to 0$ which corresponds to almost decoupled rungs. In that limit, the LEH has been derived to first order in J/J' for a three-chain ladder with PBC along the rungs,[20,24] and for a two-chain ladder.[15,25]

We will derive the LEH for the three-chain model with OBC along the rungs and a two-chain model to *second order* in J/J', and for the three-chain model with PBC along the rungs to first order. For the three-chain system with OBC and for the two-chain system, we find that the first-order LEH takes the form of the XXZ spin-1/2 model in a magnetic field. A lot of information is available for this model through conformal field theory.[11,26] In particular, the exponent η for

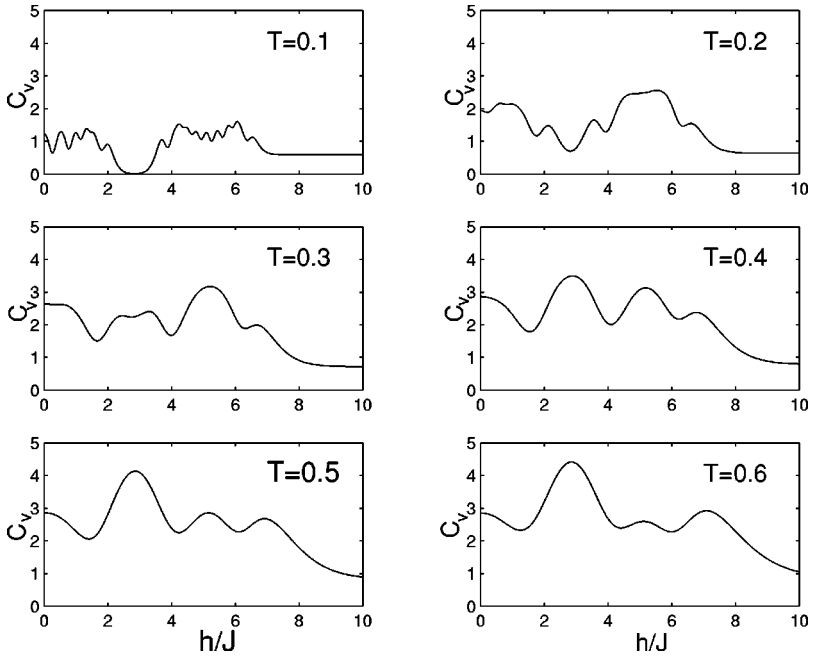

FIG. 12. Specific heat in units of k_B vs magnetic field for 36 sites, with OBC along rungs for $J/J'=1/3$.

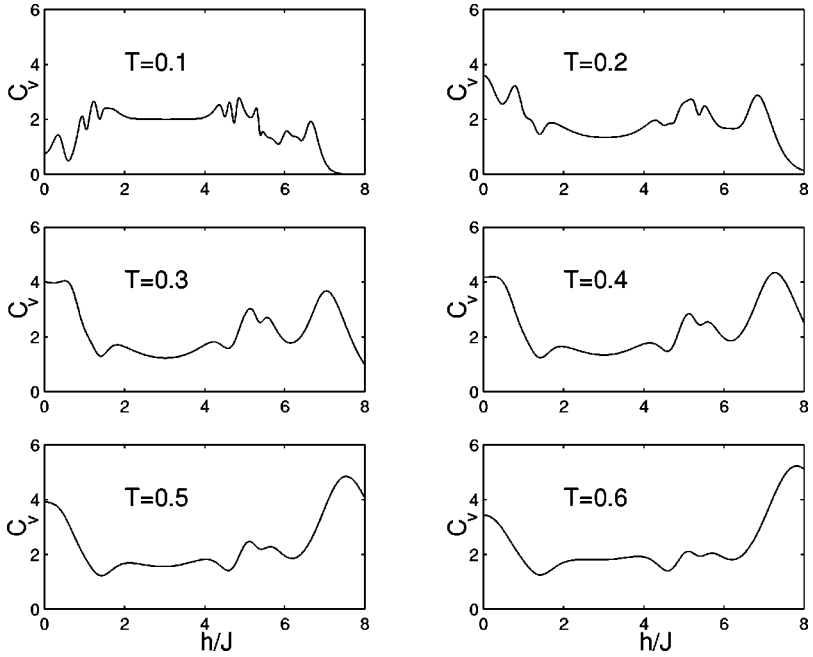

FIG. 13. Specific heat in units of k_B for 36 sites, with PBC along rungs.

the correlation power laws can be read off from the first-order Hamiltonian. We will use the terms of second order in J/J' only to determine the boundaries $h_{c\pm}$ of the various plateaus. The second-order terms should also give corrections to the exponent η but we will not consider that problem here. For the three-chain model with PBC along the rungs, even the first-order LEH is sufficiently complicated that its properties are not well understood; however we will present the form of the LEH for completeness.

We derive the LEH as follows. We first set the intrachain coupling $J=0$ and consider which of the states of a single rung are degenerate in energy in the presence of a magnetic field. In general, there will be several values of the field, denoted by h_0, for which two or more of the rung states will be degenerate ground states. We will consider each such value of h_0 in turn. The degenerate rung states will constitute our low-energy states. If the amount of degeneracy in each rung is d, the total number of low-energy states in a system with L rungs is given by L^d. (The number d depends both on the system and on the field h_0. It is two for three chains with OBC along the rungs and for two chains, while it is three or four for three chains with PBC along the rungs. The form of the LEH depends crucially on this degeneracy.) Next, we decompose the Hamiltonian of the total system as $H=H_0+V$, where H_0 contains only the rung interaction J' and the field h_0, and V contains the small interactions J and the re-

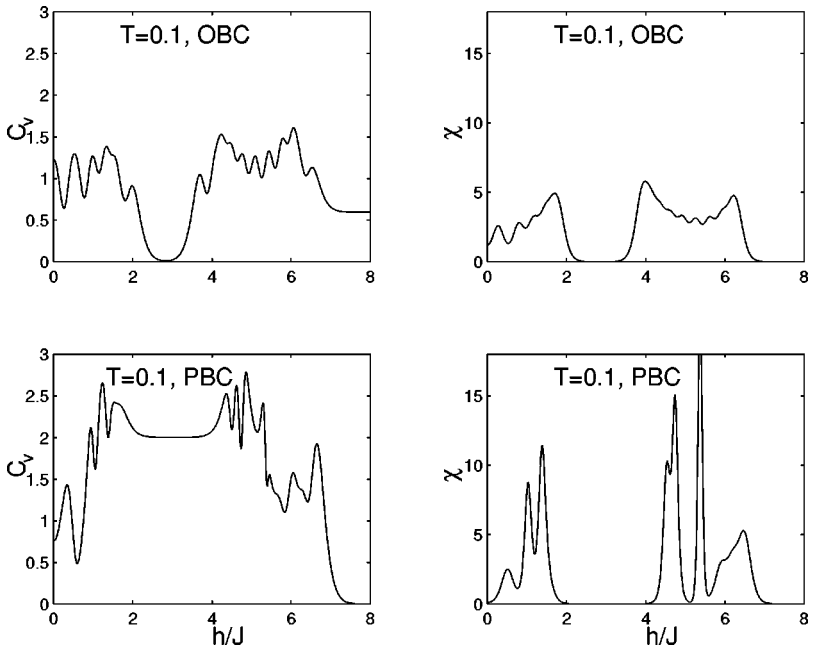

FIG. 14. Comparisons of specific heat and susceptibility of the 36-site systems with OBC and PBC along the rungs.

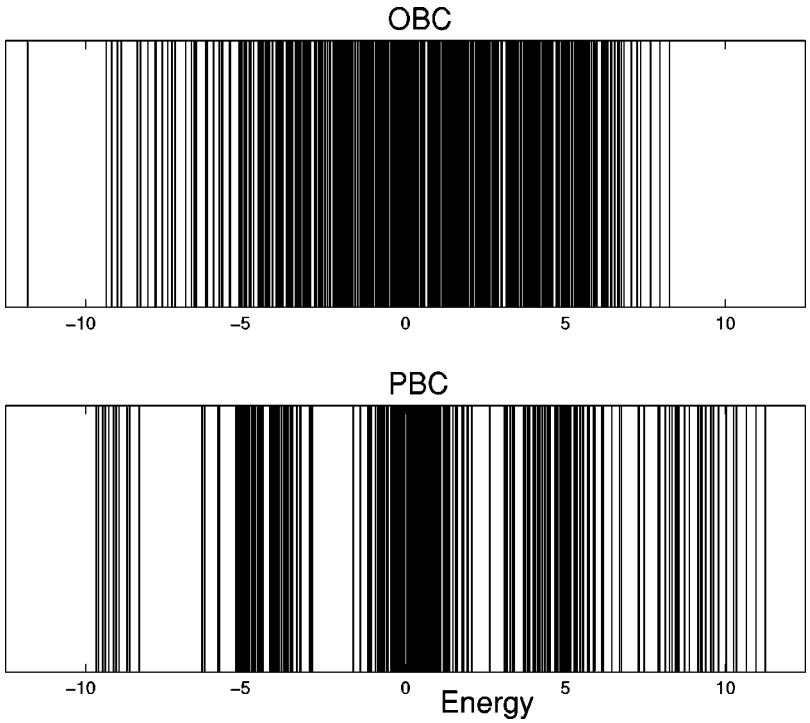

FIG. 15. Comparison of the energy spectra in units of J of the 12-site system with OBC and PBC along the rungs. The energies in the $S_z=2$ sector are shown for $J/J'=1/3$.

sidual magnetic field $h-h_0$ which are both assumed to be much smaller than J'. Let us now denote the degenerate and low-energy states of the system as p_i and the high-energy states as q_α. The low-energy states all have energy E_0, while the high-energy states have energies E_α according to the exactly solvable Hamiltonian H_0. Then the first-order LEH is given, up to an overall constant, by degenerate perturbation theory,

$$H_{\rm eff}^{(1)}=\sum_{ij}\ |p_i\rangle\langle p_i|V|p_j\rangle\langle p_j|. \tag{13}$$

The second-order LEH is given by

$$H_{\rm eff}^{(2)}=\sum_{ij}\ \sum_{\alpha}\ |p_i\rangle\frac{\langle p_i|V|q_\alpha\rangle\langle q_\alpha|V|p_j\rangle}{E_0-E_\alpha}\langle p_j|. \tag{14}$$

The calculation of the various matrix elements in Eqs. (13) and (14) can be simplified by using the symmetries of the perturbation V, e.g., translations and rotations about the $\hat{z}$ axis.

Finally, if there is a state p_i such that $\langle p_j|V|p_i\rangle=0$ for all low-energy states $j\neq i$, then the unnormalized state p_i is given, to first order, by

$$|p_i\rangle^{(1)}=|p_i\rangle+\sum_{\alpha}\ |q_\alpha\rangle\frac{\langle q_\alpha|V|p_i\rangle}{E_0-E_\alpha}. \tag{15}$$

This result will be used to compute the first-order changes in some quantities like the spin densities and correlations.

Before ending this section, we would like to make a few comments on the XXZ spin-1/2 model in a magnetic field since this will play an important role below.[11,26] Consider a spin-1/2 chain governed by the Hamiltonian

$$H=\sum_n\ [S_n^xS_{n+1}^x+S_n^yS_{n+1}^y+\Delta S_n^zS_{n+1}^z]-h\sum_n\ S_n^z, \tag{16}$$

where the anisotropy parameter $\Delta>-1$. It is known that this system is gapped for $h>1+\Delta$ with all sites having $S_z=1/2$ in the ground state, and for $h<-1-\Delta$ with all sites having $S_z=-1/2$. For $\Delta\leqslant 1$, these are the only two magnetization plateaus with $m=\pm 1/2$ per site. For $\Delta\leqslant 1$ and $h=0$, the two-spin correlations decay asymptotically as

$$\langle S_0^+S_n^-\rangle\sim\frac{(-1)^n}{|n|^\eta},$$

$$\langle S_0^zS_n^z\rangle\sim\frac{(-1)^n}{|n|^{1/\eta}}, \tag{17}$$

$$\eta=\frac{1}{2}+\frac{1}{\pi}\sin^{-1}(\Delta).$$

On the other hand, for $\Delta>1$, there is an additional plateau at $m_s=0$; there are two degenerate ground states which have a period of two sites consistent with the condition (1). Thus the invariance of the Hamiltonian under a translation by one site is spontaneously broken in the ground states. This is particularly obvious for $\Delta\to\infty$ where the two ground states are $+-+-\cdots$ and $-+-+\cdots$. The two-spin correlations decay exponentially for $\Delta>1$ and $h=0$.

B. Three-chain ladder with open boundary condition along the rungs

We will decompose the Hamiltonian in Eq. (2) as $H=H_0+V$, where

$$H_0 = J' \sum_{a=1,2} \sum_n \mathbf{S}_{a,n} \cdot \mathbf{S}_{a+1,n} - h_0 \sum_{a=1}^{3} \sum_n S^z_{a,n},$$

$$V = J \sum_{a=1}^{3} \sum_n \mathbf{S}_{a,n} \cdot \mathbf{S}_{a,n+1} - (h - h_0) \sum_{a=1}^{3} \sum_n S^z_{a,n}. \tag{18}$$

We determine the field h_0 by considering the rung Hamiltonian H_0 and identifying the values of the magnetic field h_0 where two or more of the rung states become degenerate.

The eight states in each rung are described by specifying the S^z components (+ and − denoting $+1/2$ and $-1/2$, respectively) of the sites belonging to chains 1, 2, and 3. For instance, the four states with total $S=3/2$ are denoted by $|1\rangle$, ..., $|4\rangle$, where $|1\rangle = |+++\rangle$ and the other three states can be obtained by acting on it successively with the operator $S^- = \Sigma_a S^-_a$. These four states have the energy $J'/2$ in the absence of a magnetic field. There is one doublet of states $|5\rangle$ and $|6\rangle$ with $S=1/2$, where $|5\rangle = [2|+--\rangle - |-++\rangle - |+-+\rangle]/\sqrt{6}$ and $|6\rangle \sim S^-|5\rangle$. These have energy $-J'$. Finally, there is another doublet of states $|7\rangle = [|+-+\rangle - |-++\rangle]/\sqrt{2}$ and $|8\rangle \sim S^-|7\rangle$ which have zero energy. It is now evident that the state $|1\rangle$ with $S^z=3/2$ and the state $|5\rangle$ with $S^z=1/2$ become degenerate at a magnetic field $h_0 = 3J'/2$, while states $|5\rangle$ and $|6\rangle$ are trivially degenerate for the field $h_0=0$. We will now examine these two cases separately.

For $h_0 = 3J'/2$, the low-energy states in each rung are given by $|1\rangle$ and $|5\rangle$, while the other six are high-energy states. We thus have an effective spin-1/2 object on each rung n. We may introduce three spin-1/2 operators (S^x_n, S^y_n, S^z_n) for each rung such that $S^{\pm}_n = S^x_n \pm i S^y_n$ and S^z_n have the following actions:

$$S^+_n |1\rangle_n = 0, \quad S^+_n |5\rangle_n = |1\rangle_n,$$

$$S^-_n |1\rangle_n = |5\rangle_n, \quad S^-_n |5\rangle_n = 0, \tag{19}$$

$$S^z_n |1\rangle_n = \tfrac{1}{2} |1\rangle_n, \quad S^z_n |5\rangle_n = -\tfrac{1}{2} |5\rangle_n.$$

Note that the state which has a $|1\rangle$ on every rung, i.e., $|111\cdots\rangle$, is just the state with rung magnetization $m_s = 3/2$ corresponding to the saturation plateau. The state with a $|5\rangle$ on every rung corresponds to the $m_s = 1/2$ magnetization plateau. The LEH we are trying to derive will therefore describe the transition between these two plateaus.

We now turn on the perturbation V in Eq. (18) with the assumption that J and $h - h_0$ are both much smaller than J'. We can write $V = \Sigma_n V_{n,n+1}$, where

$$V_{n,n+1} = J \sum_{a=1}^{3} \mathbf{S}_{a,n} \cdot \mathbf{S}_{a,n+1} - \frac{1}{2}(h - h_0) \sum_{a=1}^{3} [S^z_{a,n} + S^z_{a,n+1}]. \tag{20}$$

The action of $V_{n,n+1}$ on the four low-energy states involving rungs n and $n+1$ can be obtained after a long but straightforward calculation. We then use Eq. (14) and find that the LEH to second order in J/J' is given, up to a constant, by

$$H_{\text{eff}} = J \sum_n \left[S^x_n S^x_{n+1} + S^y_n S^y_{n+1} + \left(\frac{1}{2} - \frac{29J}{72J'} \right) S^z_n S^z_{n+1} \right] - \frac{5J^2}{18J'} \sum_n \left(\frac{1}{2} - S^z_n \right) (S^x_{n-1} S^x_{n+1} + S^y_{n-1} S^y_{n+1}) - \frac{2J^2}{27J'} \sum_n \left(\frac{1}{2} - S^z_{n-1} \right) \left(\frac{1}{2} - S^z_n \right) \left(\frac{1}{2} - S^z_{n+1} \right) - \left(h - \frac{3J'}{2} - \frac{J}{2} - \frac{29J^2}{72J'} \right) \sum_n S^z_n, \tag{21}$$

where we have substituted $h_0 = 3J'/2$. Note that the terms of order J only involve two neighboring sites. The LEH up to that order simply describes an XXZ model with anisotropy $\Delta = 1/2$ in a magnetic field $h - 3J'/2 - J/2$ [see Eq. (16)]. Some of the terms of order J^2/J' involve three neighboring sites; this makes the model unsolvable by the Bethe ansatz at this order.

We will now use Eq. (21) to compute the values of the fields h_1 and h_2 where the states with all rungs equal to $|1\rangle$ and all rungs equal to $|5\rangle$, respectively, become the ground states. We can then identify h_1 with the lower critical field h_{c-} for the plateau at $m_s = 3/2$, and h_2 with the upper critical field h_{c+} for the plateau at $m_s = 1/2$. [Recall the definition of upper and lower critical fields around Eqs. (4) and (5).]

To compute the field h_1, we compare the energy E_0 of the state with all rungs equal to $|1\rangle$ with the minimum energy $E_{\min}(k)$ of a spin-wave state in which one rung is equal to $|5\rangle$ and all the other rungs are equal to $|1\rangle$. A spin wave with momentum k is given by

$$|k\rangle = \frac{1}{\sqrt{L}} \sum_n e^{ikn} |5_n\rangle, \tag{22}$$

where $|5_n\rangle$ denotes a state where only the rung n is equal to $|5\rangle$. The spin-wave dispersion, i.e., $\omega(k) = E(k) - E_0$, is found from Eq. (21) to be

$$\omega(k) = J \left(\cos k - \frac{1}{2} + \frac{29J}{72J'} \right) + \left(h - \frac{3J'}{2} - \frac{J}{2} - \frac{29J^2}{J'} \right). \tag{23}$$

This is minimum at $k = \pi$ and it turns negative there for $h < h_1$, where

$$h_1 = \frac{3J'}{2} + 2J. \tag{24}$$

This is therefore the transition point between the ferromagnetic state $|111\cdots\rangle$ and a spin-wave band lying immediately below it in energy.

Similarly, we compute the field h_2 by comparing the energy E_0 of the state with all rungs equal to $|5\rangle$ with the minimum energy $E_{\min}(k)$ of a spin wave in which a $|5\rangle$ at one rung is replaced by a $|1\rangle$. For a spin wave with momentum k, the dispersion $\omega(k) = E(k) - E_0$ is found to be

$$\omega(k)=J\left(\cos k-\frac{1}{2}+\frac{29J}{72J'}\right)+\frac{J^2}{J'}\left(\frac{2}{9}-\frac{5}{18}\cos 2k\right)-\left(h-\frac{3J'}{2}-\frac{J}{2}-\frac{29J^2}{72J'}\right). \quad (25)$$

This is minimum at $k=\pi$ and it turns positive there for $h>h_2$, where

$$h_2=\frac{3J'}{2}-J+\frac{3J^2}{4J'}. \quad (26)$$

This marks the transition between the state $|555\cdots\rangle$ and the spin-wave band. Equation (26) agrees to this order with the higher-order series given in the literature.[11] Note that the second-order result gives $h_2/J=3.75$ for $J/J'=1/3$, compared to our DMRG value of $h_{c+}/J=3.79$ in Eq. (6).

From the first-order terms in Eq. (21), we can deduce the asymptotic form of the two-spin correlations. From Eq. (17), we see that the exponent $\eta=2/3$ for $\Delta=1/2$. Although this is the exponent for the $+-$ correlation of the effective spin-1/2 defined on each rung, we would expect the same exponent to appear in all the correlations $\langle S^+_{a,l}S^-_{b,n}\rangle$ studied by DMRG in the previous section, regardless of how we choose the chain indices $a,b=1,2,3$. We now see that the analytically predicted exponent of 2/3 agrees quite well with the numerically obtained exponents which lie in the range 0.61 to 0.70. Incidentally, this agreement implies that $J/J'=1/3$ is sufficiently small so that the second-order terms do not significantly affect the correlation exponent.

Finally, we can use the first-order wave function given in Eq. (15) to compute the spin densities and short-distance two-spin correlations. As examples, we quote the results for spin densities and some of the nearest-neighbor spin correlations for the plateau at $m_s=1/2$. We will give the first-order expressions and their values for $J/J'=1/3$, followed by the numerical values obtained by DMRG:

$$\langle S^z_{1,n}\rangle=\langle S^z_{3,n}\rangle=\frac{1}{3}-\frac{4J}{27J'}=0.28 \text{ vs } 0.27 \text{ from DMRG},$$

$$\langle S^z_{2,n}\rangle=-\frac{1}{6}+\frac{8J}{27J'}=-0.07 \text{ vs } -0.04,$$

$$\langle S^z_{1,n}S^z_{1,n+1}\rangle=\frac{1}{9}-\frac{J}{8J'}=0.07 \text{ vs } 0.07,$$

$$\langle S^z_{2,n}S^z_{2,n+1}\rangle=\frac{1}{36}-\frac{4J}{27J'}=-0.02 \text{ vs } -0.02,$$

$$\langle S^+_{1,n}S^-_{1,n+1}\rangle=-\frac{J}{6J'}=-0.06 \text{ vs } -0.08,$$

$$\langle S^+_{2,n}S^-_{2,n+1}\rangle=-\frac{2J}{9J'}=-0.07 \text{ vs } -0.11. \quad (27)$$

We will now consider the LEH at the other magnetic field $h_0=0$ where the rung states $|5\rangle$ and $|6\rangle$ are degenerate. We take these as the low-energy states and introduce new effective spin-1/2 operators for each rung with actions similar to Eqs. (19), except that we replace $|1\rangle$ and $|5\rangle$ in those equations by $|5\rangle$ and $|6\rangle$. We again compute the action of the perturbation V on the low-energy states. We then deduce the second-order LEH to be

$$H_{\rm eff}=J\sum_n\left[\left(1-\frac{J}{9J'}\right)\mathbf{S}_n\cdot\mathbf{S}_{n+1}-\frac{8J}{27J'}\mathbf{S}_n\cdot\mathbf{S}_{n+2}\right]-h\sum_n S^z_n. \quad (28)$$

This Hamiltonian describes the transition between the magnetization plateaus at $m_s=1/2$ and $m_s=-1/2$; since these plateaus are reflections of each other about zero magnetic field, it is sufficient to study one of them. By a calculation similar to the one used to derive Eq. (24), the field h_1 can be found from the dispersion of a spin wave in which one rung is equal to $|6\rangle$ and all the other rungs are equal to $|5\rangle$. The dispersion is

$$\omega(k)=h+\left(J-\frac{J^2}{9J'}\right)(\cos k-1)+\frac{8J^2}{27J'}(1-\cos 2k). \quad (29)$$

This gives

$$h_1=2J-\frac{2J^2}{9J'}. \quad (30)$$

This is the lower critical field h_{c-} of the $m_s=1/2$ plateau. For $J/J'=1/3$, the second-order result gives 1.93 versus the DMRG value of 1.91 in Eq. (6). The Hamiltonian (28) describes an isotropic spin-1/2 antiferromagnet with a weak ferromagnetic next-nearest-neighbor interaction. From the comments at the end of the previous section, we see that this model only has the two saturation plateaus at $m_s=\pm 1/2$, and no other plateau in between. For $h=0$, the two-spin correlations decay as power laws with the exponent $\eta=1$ [see Eq. (17)].

C. Three-chain ladder with periodic boundary condition along the rungs

In this section, we will present the first order LEH for the Hamiltonian (2) with PBC along the rungs. The LEH will turn out to be somewhat complicated. We will not study their properties in any detail, but will limit ourselves to a few comments. As in the case with OBC along the rungs, there are two different LEH to be considered here because there are two values of the magnetic field where there are degeneracies. We again begin with a description of the eight states on each rung. The four states with $S=3/2$ are the same as the states $|1\rangle$, ..., $|4\rangle$ introduced in the previous section, except that they now have energy $3J'/4$ in the absence of a field. The doublet states have to be chosen differently now in order that they be eigenstates of the periodic rung Hamiltonian. We choose two of the doublet states to be $|5'\rangle=[|++-\rangle$

$+\omega^2|+-+\rangle+\omega|-++\rangle]/\sqrt{3}$ and $|6'\rangle \sim S^-|5'\rangle$, where $\omega = \exp(i2\pi/3)$. These two states have momenta $2\pi/3$ along the rung (right moving). The other two doublet states are $|7'\rangle=[|++-\rangle+\omega|+-+\rangle+\omega^2|-++\rangle]/\sqrt{3}$ and $|8'\rangle \sim S^-|7'\rangle$ with momenta $-2\pi/3$ (left moving). All these four states have energy $-3J'/4$. This extra degeneracy (which is twice the degeneracy of the doublets for OBC along the rungs) leads to a more complicated LEH as we will see.

We now note that for a field $h_0=3J'/2$, the three states $|1\rangle$, $|5'\rangle$, and $|7'\rangle$ become degenerate. We now introduce seven operators $R^{\pm}, L^{\pm}, \tau^{\pm}$, and σ^z for each rung with the following nonzero actions on the three low-energy states,

$$R_n^+|5'\rangle_n=|1\rangle_n, \quad R_n^-|1\rangle_n=|5'\rangle_n,$$

$$L_n^+|7'\rangle_n=|1\rangle_n, \quad L_n^-|1\rangle_n=|7'\rangle_n,$$

$$\tau_n^+|7'\rangle_n=|5'\rangle_n, \quad \tau_n^-|5'\rangle_n=|7'\rangle_n,$$

$$\sigma_n^z|1\rangle_n=|1\rangle_n, \quad \sigma_n^z|5'\rangle_n=-|5'\rangle_n, \quad \sigma_n^z|7'\rangle_n=-|7'\rangle_n. \tag{31}$$

All the actions (of operators on states) not mentioned in Eqs. (31) are assumed to give zero. We thus observe that there are five magnetic operators $L^{\pm}$, $R^{\pm}$, and σ^z which change or measure the S^z of a state, and two nonmagnetic operators $\tau^{\pm}$ which do not change S^z but simply interchange the right and left moving states.

We then find that the first-order LEH is given, up to a constant, by

$$H_{\rm eff}=\frac{J}{2}\sum_n [L_n^+L_{n+1}^- + L_n^-L_{n+1}^+ + R_n^+R_{n+1}^- + R_n^-R_{n+1}^+] + \frac{J}{3}\sum_n [\tau_n^+\tau_{n+1}^- + \tau_n^-\tau_{n+1}^+] + \frac{J}{12}\sum_n \sigma_n^z\sigma_{n+1}^z - \frac{1}{2}\left(h-\frac{3J'}{2}-\frac{2J}{3}\right)\sum_n \sigma_n^z. \tag{32}$$

We can now find the magnetic field h_1 at which the ferromagnetic state $|111\cdots\rangle$ crosses over to the minimum energy spin-wave state (in which a $|1\rangle$ is replaced by either a $|5'\rangle$ or a $|7'\rangle$ on exactly one rung). The spin-wave dispersion is

$$\omega(k)=h-\frac{3J'}{2}-J+J\cos k. \tag{33}$$

We thus see that $h_1=3J'/2+2J$ just as for OBC along the rungs. Thus the lower critical field h_{c-} of the saturation plateau $m_s=3/2$ has the same value for OBC and PBC along the rungs.

Below some field h_2 (which seems rather hard to find analytically), the low-energy eigenstates of Eq. (32) will not have the state $|1\rangle$ on any rung; only the states $|5'\rangle$ and $|7'\rangle$ will appear. This gives us the magnetization plateau $m_s=1/2$. However, this plateau has a large number of *nonmagnetic* excitations described by the Hamiltonian

$$H_{\rm eff}=\frac{J}{3}\sum_n [\tau_n^+\tau_{n+1}^- + \tau_n^-\tau_{n+1}^+], \tag{34}$$

which may be obtained from Eq. (32) by omitting the state $|1\rangle$ on all the rungs. Equation (34) has the form of Eq. (16) with $\Delta=0$, and is therefore exactly solvable; at low temperature, it has a specific heat which grows linearly with T. The situation is therefore quite different from the case of OBC along the rungs where the $m_s=1/2$ plateau consists of a single state in which every rung is in the state $|5\rangle$; all other states are separated by a gap, hence the specific heat goes to zero exponentially at low temperature.

Finally, we examine the LEH at the field $h_0=0$ where the four doublet states $|5'\rangle,\cdots,|8'\rangle$ become degenerate. This has been discussed in detail earlier.[11,20,24] On each rung, we introduce effective spin-1/2 operators which change or measure S^z, and the two nonmagnetic operators $\tau^{\pm}$ which interchange the left and right moving states. Then the LEH is

$$H_{\rm eff}=\frac{J}{3}\sum_n [1+4(\tau_n^+\tau_{n+1}^- + \tau_n^-\tau_{n+1}^+)] \times \mathbf{S}_n\cdot\mathbf{S}_{n+1} - h\sum_n S_n^z. \tag{35}$$

This also appears to be nonexactly solvable but it has been studied numerically.[11,24] It has a small plateau at $m_s=0$ where there are two degenerate ground states, each with a period of two rungs. Above some magnetic field h_1 (which is again hard to calculate analytically from Eq. (35), this model crosses over to the $m_s=1/2$ plateau where the rungs can only be in the two $S^z=1/2$ states $|5'\rangle$ and $|7'\rangle$. We see from Eq. (35) that these two states are again governed by the Hamiltonian in Eq. (34).

The phase diagrams of the three-chain ladder for OBC and PBC along the rungs are shown as functions of J'/J and h/J in Figs. 6(b) and 6(c) in Ref. 11. We observe that the plateaus with $m_s=1/2$ and $m_s=3/2$ (called $M=1/3$ and $M=1$, respectively, in Ref. 11) have large regions of stability for both OBC and PBC. The plateau with $m_s=0$ exists only in the case of PBC along the rungs, and it has a small region of stability close to $h/J=0$.

D. A two-chain ladder

In this section, we will use the LEH approach to study a two-chain spin-1/2 ladder with the following Hamiltonian:

$$H=J'\sum_n \mathbf{S}_{1,n}\cdot\mathbf{S}_{2,n} + J_2\sum_{a=1}^{2}\sum_n \mathbf{S}_{a,n}\cdot\mathbf{S}_{a,n+1} + 2J_1\sum_n \mathbf{S}_{1,n}\cdot\mathbf{S}_{2,n+1} - h\sum_{a=1}^{2}\sum_n S_{a,n}^z, \tag{36}$$

as shown in Fig. 16. The model may be viewed as a single

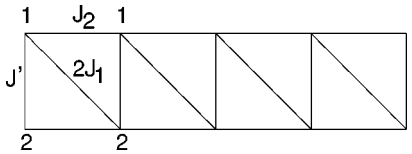

FIG. 16. Schematic diagram of the two-chain ladder with an additional diagonal interaction. The labels 1 and 2 denote sites in the upper and lower chains, respectively.

chain with an alternation in nearest-neighbor couplings J' and $2J_1$ (dimerization), and a next-nearest-neighbor coupling J_2 (frustration). Equation (36) has been studied extensively.[27,29] More recently, it has been studied from the point of view of magnetization plateaus using a first-order LEH, bosonization, and exact diagonalization.[15,16,25] We will therefore limit ourselves to deriving the second-order LEH and making a few other comments.

We begin by setting $J_1=J_2=0$, and studying the four states on each rung. These are specified by giving the configurations $\pm$ of the spins on chains 1 and 2 as follows. The three triplet states with $S=1$ are denoted as $|1\rangle$, $|2\rangle$, and $|3\rangle$, where $|1\rangle=|++\rangle$ and the other two states are obtained by acting on it successively with S^-. These three states have energy $J'/4$ in the absence of a magnetic field. The singlet state $|4\rangle=[|+-\rangle-|-+\rangle]/\sqrt{2}$ has energy $-3J'/4$. The states $|1\rangle$ and $|4\rangle$ become degenerate at a field $h_0=J'$. We now develop perturbation theory by assuming that J_1, J_2 and $h-h_0$ are all much less than J'. The perturbation is $V=\Sigma_n V_{n,n+1}$ where

$$V_{n,n+1}=J_2\sum_{a=1}^{2}\mathbf{S}_{a,n}\cdot\mathbf{S}_{a,n+1}+2J_1\mathbf{S}_{1,n}\cdot\mathbf{S}_{2,n+1}-\frac{1}{2}(h-h_0)\sum_{a=1}^{2}[S^z_{a,n}+S^z_{a,n+1}]. \tag{37}$$

The actions of this operator on the four low-energy states of a pair of neighboring rungs can be easily obtained. We now introduce effective spin-1/2 operators $\mathbf{S}_n$ on each rung which act on the two low-energy states. The second-order LEH is then found to be

$$\begin{aligned}H_{\rm eff}=&\left(J_2-J_1-\frac{J_1^2}{J'}\right)\sum_n(S^x_nS^x_{n+1}+S^y_nS^y_{n+1})+\frac{1}{2}\left(J_2+J_1+\frac{2J_1^2}{J'}-\frac{3(J_1-J_2)^2}{4J'}\right)\sum_n S^z_nS^z_{n+1}\\&+\frac{J_1^2}{2J'}\sum_n\left[\left(\frac{1}{2}+S^z_n\right)(S^x_{n-1}S^x_{n+1}+S^y_{n-1}S^y_{n+1})+\left(\frac{1}{2}+S^z_{n-1}\right)(S^x_nS^x_{n+1}+S^y_nS^y_{n+1})\right.\\&\left.+\left(\frac{1}{2}+S^z_{n+1}\right)(S^x_{n-1}S^x_n+S^y_{n-1}S^y_n)+\left(\frac{1}{2}+S^z_{n-1}\right)\left(\frac{1}{2}-S^z_n\right)\left(\frac{1}{2}+S^z_{n+1}\right)\right]\\&-\frac{(J_1-J_2)^2}{4J'}\sum_n\left(\frac{1}{2}-S^z_n\right)(S^x_{n-1}S^x_{n+1}+S^y_{n-1}S^y_{n+1})-\left(h-J'-\frac{J_1}{2}-\frac{J_2}{2}-\frac{3(J_1-J_2)^2}{8J'}\right)\sum_n S^z_n.\end{aligned} \tag{38}$$

We now compute the field h_1 above which the state $|111\cdots\rangle$ becomes the ground state. The dispersion of a spin wave, in which one rung is equal to $|4\rangle$ and all the others are equal to $|1\rangle$, is given by

$$\omega(k)=h-J'-J_1-J_2-\frac{J_1^2}{2J'}+(J_2-J_1)\cos k+\frac{J_1^2}{2J'}\cos 2k. \tag{39}$$

By minimizing this as a function of k in various regions in the parameter space (J_1,J_2), and then setting that minimum value equal to zero, we find that h_1 is given by

$$\begin{aligned}h_1&=J'+2J_1\ \text{ if }\ J_2\leqslant J_1-\frac{2J_1^2}{J'},\\&=J'+J_1+J_2+\frac{J_1^2}{J'}+\frac{(J_1-J_2)^2J'}{4J_1^2}\\&\quad\text{if }\ J_1-\frac{2J_1^2}{J'}\leqslant J_2\leqslant J_1+\frac{2J_1^2}{J'},\\&=J'+2J_2\ \text{ if }\ J_2\geqslant J_1+\frac{2J_1^2}{J'}.\end{aligned} \tag{40}$$

This is the lower critical field h_{c-} of the saturation plateau with magnetization $m_s=1$ per rung. Similarly, we can find the field h_2 from the dispersion of a spin wave in which one rung is equal to $|1\rangle$ and the rest are equal to $|4\rangle$. The dispersion is given by

$$\omega(k)=-h+J'+\frac{3(J_1-J_2)^2}{4J'}-\frac{J_1^2}{J'}+\left(J_2-J_1-\frac{J_1^2}{J'}\right)\cos k-\frac{(J_1-J_2)^2}{4J'}\cos 2k. \tag{41}$$

By setting the minimum of this equal to zero, we find that h_2 is given by

$$\begin{aligned}h_2&=J'+\frac{(J_1-J_2)^2}{2J'}+J_2-J_1-\frac{2J_1^2}{J'}\ \text{ if }\ J_2\leqslant J_1+\frac{J_1^2}{J'},\\&=J'+\frac{(J_1-J_2)^2}{2J'}-J_2+J_1\ \text{ if }\ J_2\geqslant J_1+\frac{J_1^2}{J'}.\end{aligned} \tag{42}$$

This is the upper critical field h_{c+} of the saturation plateau with magnetization $m_s=0$ per rung.

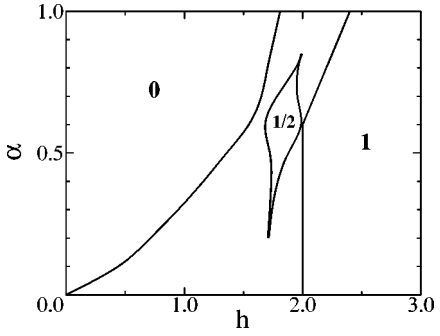

FIG. 17. Phase diagram of the two-chain ladder as a function of h and α for $J_2=0.2$. In our notation, $J'=1+\alpha$ and $2J_1=1-\alpha$. The numbers 0, 1/2, and 1 in the figure correspond to the values of m_s at the plateaus. Reproduced with permission from Ref. 16.

Finally, we can see that the first-order terms in Eq. (38) are of the same form as the XXZ model in Eq. (16). We can always make the coefficient of the first term in Eq. (38) positive, if necessary by performing a rotation $S_n^x \rightarrow (-1)^n S_n^x$, $S_n^y \rightarrow (-1)^n S_n^y$ and $S_n^z \rightarrow S_n^z$. We then get a first-order Hamiltonian of the form

$$H_{\text{eff}}=|J_2-J_1|\sum_n \left[S_n^x S_{n+1}^x+S_n^y S_{n+1}^y\right] + \frac{1}{2}(J_2+J_1)\sum_n S_n^z S_{n+1}^z-\left(h-J'-\frac{J_1}{2}-\frac{J_2}{2}\right)\sum_n S_n^z. \tag{43}$$

This is an XXZ model with

$$\Delta=\frac{J_2+J_1}{2|J_2-J_1|}. \tag{44}$$

From the comments in Sec. III A, we therefore see that the two-chain ladder will have an additional plateau at $m_s=1/2$ for $\Delta>1$, i.e., if $J_2+J_1>2|J_2-J_1|$. In particular, $\Delta=\infty$ for $J_2=J_1$ (this is called the Shastry-Sutherland line[30]); the $m_s=1/2$ plateau will then stretch all the way from the upper critical field of the $m_s=0$ plateau to the lower critical field of the $m_s=1$ plateau. This can be seen in Fig. 17 which is taken from Ref. 16; the dimerization parameter α in that figure is related to our couplings by $J'=1+\alpha$ and $2J_1=1-\alpha$. Note that the $m_s=1/2$ plateau is particularly broad at $\alpha=0.6$, i.e., $J_2=J_1=0.2$, and that it actually touches the $m_s=1$ plateau on the right. The fact that it does not extend all the way up to the $m_s=0$ plateau on the left is probably because we have ignored the second-order terms in Eq. (38) which lead to deviations from the XXZ model.

IV. SUMMARY AND OUTLOOK

We studied a three-chain spin-1/2 ladder with a large ratio of interchain coupling to intrachain coupling using the DMRG method and a LEH approach. For both OBC and PBC along the rungs, we found a wide plateau with rung magnetization given by $m_s=1/2$. For the case of OBC, the two-spin correlations are extremely short-ranged, and the magnetic susceptibility and specific heat are very small at low temperature in the plateau. All these are consistent with the large magnetic gap. At other values of m, the two-spin correlations fall off as power laws; the exponents can be found by using the first-order LEH which takes the form of an XXZ model in a longitudinal magnetic field. For the case of PBC, the magnetic susceptibility is again very small at low temperature in the plateau. However, the specific heat goes to zero much more slowly which dramatically shows the presence of nonmagnetic excitations. This can be understood from the LEH in Eq. (34) which is an XY model. Finally, we used the LEH approach to study a two-chain ladder with an additional diagonal interaction. In addition to a plateau at $m_s=0$, this system also has a plateau at $m_s=1/2$ for certain regions in parameter space. The $m_s=1/2$ plateau is interesting because it corresponds to degenerate ground states which spontaneously break the translation invariance of the Hamiltonian. This can be understood from the LEH which, at first order, is an XXZ model with $\Delta>1$.

An interesting problem for the future may be to take the second-order terms in the LEH presented in Secs. III B and III D, and to compute the corrections produced by them in the exponents of the correlation power laws. This would require us to study the effects of a perturbation to the XXZ spin-1/2 chain. This may not be difficult to do analytically since the XXZ model is integrable and exactly solvable by the Bethe ansatz.

The quantization condition for magnetization given in Eq. (1) is reminiscent of the quantum Hall effect where the Hall conductivity shows plateaus as a function of the magnetic field.[31] However, it is not clear if the magnetization quantization is as insensitive to disorder as the conductivity quantization is known to be. Although a magnetization plateau may be expected to survive small amounts of disorder (e.g., if the disorder strength is much smaller than the energy gap), there seems to be no fundamental physical principle, analogous to gauge invariance in the quantum Hall system, why the *value* of the magnetization should remain fixed at a simple rational value. In fact, the derivation of Eq. (1) assumes translation invariance of the Hamiltonian which is certainly broken by disorder. It would therefore be interesting to study this issue, for instance, by allowing a small amount of disorder in the couplings of the spin ladder models discussed in this paper.

ACKNOWLEDGMENTS

We thank Andreas Honecker and Sriram Shastry for useful discussions. We are grateful to T. Tonegawa for giving us permission to reproduce Fig. 17 from Ref. 16. The present work has been partly supported by the Indo-French Centre for the Promotion of Advanced Research through project No. 1308-4, ''Chemistry and Physics of Molecule based Materials.''

[1] F. D. M. Haldane, Phys. Lett. **93A**, 464 (1983); , Phys. Rev. Lett. **50**, 1153 (1983).
[2] W. J. L. Buyers, R. M. Morra, R. L. Armstrong, M. J. Hogan, P. Gerlach, and K. Hirakawa, Phys. Rev. Lett. **56**, 371 (1986); J. P. Renard, M. Verdaguer, L. P. Regnault, W. A. C. Erkelens, J. Rossat-Mignod, and W. G. Stirling, Europhys. Lett. **3**, 945 (1987); S. Ma, C. Broholm, D. H. Reich, B. J. Sternlieb, and R. W. Erwin, Phys. Rev. Lett. **69**, 3571 (1992).
[3] E. Dagotto and T. M. Rice, Science **271**, 618 (1996).
[4] R. S. Eccleston, T. Barnes, J. Brody, and J. W. Johnson, Phys. Rev. Lett. **73**, 2626 (1994).
[5] M. Azuma, Z. Hiroi, M. Takano, K. Ishida, and Y. Kitaoka, Phys. Rev. Lett. **73**, 3463 (1994).
[6] G. Chaboussant, P. A. Crowell, L. P. Levy, O. Piovesana, A. Madouri, and D. Mailly, Phys. Rev. B **55**, 3046 (1997).
[7] M. Hase, I. Terasaki, and K. Uchinokura, Phys. Rev. Lett. **70**, 3651 (1993); M. Nishi, O. Fujita, and J. Akimitsu, Phys. Rev. B **50**, 6508 (1994); G. Castilla, S. Chakravarty, and V. J. Emery, Phys. Rev. Lett. **75**, 1823 (1995).
[8] G. Chaboussant, Y. Fagot-Revurat, M.-H. Julien, M. E. Hanson, C. Berthier, M. Horvatic, L. P. Levy, and O. Piovesana, Phys. Rev. Lett. **80**, 2713 (1998).
[9] M. Oshikawa, M. Yamanaka, and I. Affleck, Phys. Rev. Lett. **78**, 1984 (1997).
[10] D. C. Cabra, A. Honecker, and P. Pujol, Phys. Rev. Lett. **79**, 5126 (1997).
[11] D. C. Cabra, A. Honecker, and P. Pujol, Phys. Rev. B **58**, 6241 (1998).
[12] K. Hida, J. Phys. Soc. Jpn. **63**, 2359 (1994).
[13] T. Kuramoto, cond-mat/9710229 (unpublished).
[14] K. Totsuka, Phys. Lett. A **228**, 103 (1997).
[15] K. Totsuka, Phys. Rev. B **57**, 3454 (1998).
[16] T. Tonegawa, T. Nishida, and M. Kaburagi, cond-mat/9712297 Physica B (to be published).
[17] T. Sakai and M. Takahashi, Phys. Rev. B **57**, R3201 (1998).
[18] T. Sakai and M. Takahashi, Phys. Rev. B **57**, 8091 (1998).
[19] R. Chitra and T. Giamarchi, Phys. Rev. B **55**, 5816 (1997).
[20] H. J. Schulz, in *Strongly Correlated Magnetic and Superconducting Systems*, edited by G. Sierra and M. A. Martin-Delgado, Lecture Notes in Physics 478 (Springer, Berlin, 1997).
[21] I. Affleck, in *Fields, Strings, and Critical Phenomena*, edited by E. Brezin and J. Zinn-Justin (North-Holland, Amsterdam, 1989).
[22] M. Reigrotzki, H. Tsunetsugu, and T. M. Rice, J. Phys.: Condens. Matter **6**, 9235 (1994); T. Barnes, J. Riera, and D. A. Tennant, cond-mat/9801224 (unpublished).
[23] S. R. White, Phys. Rev. Lett. **69**, 2863 (1992); Phys. Rev. B **48**, 10 345 (1993).
[24] K. Kawano and M. Takahashi, J. Phys. Soc. Jpn. **66**, 4001 (1997).
[25] F. Mila, cond-mat/9805029 (unpublished); A. K. Kolezhuk, cond-mat/9806292, Phys. Rev. B (to be published).
[26] F. D. M. Haldane, Phys. Rev. Lett. **45**, 1358 (1980).
[27] R. Chitra, S. K. Pati, H. R. Krishnamurthy, D. Sen, and S. Ramasesha, Phys. Rev. B **52**, 6581 (1995).
[28] S. K. Pati, S. Ramasesha, and D. Sen, Phys. Rev. B **55**, 8894 (1997); J. Phys.: Condens. Matter **9**, 8707 (1997).
[29] P. R. Hammar and D. H. Reich, J. Appl. Phys. **79**, 5392 (1996); C. A. Hayward, D. Poilblanc, and L. P. Levy, Phys. Rev. B **54**, R12 649 (1996).
[30] B. S. Shastry and B. Sutherland, Phys. Rev. Lett. **47**, 964 (1981).
[31] R. E. Prange and S. M. Girvin, *The Quantum Hall Effect* (Springer, Berlin, 1986).